Eur. Phys. J. C (2026) 86:212
https://doi.org/10.1140/epjc/s10052-026-15457-x

THE EUROPEAN PHYSICAL JOURNAL C

Regular Article - Theoretical Physics

Greybody factor for accelerating rotating BTZ black hole

Jamil Ahmed[1,a], **Usman A. Gillani**[2,b], **Mudassar Rehman**[3,c]

[1] Pak Austria Fachhochschule: Institute of Applied Sciences and Technology, Haripur, Pakistan
[2] National University of Technology, Islamabad, Pakistan
[3] Department of Mathematics, Quaid-i-Azam University, Islamabad, Pakistan

Received: 10 December 2025 / Accepted: 16 February 2026

Abstract We investigate the greybody factor for the accelerating rotating Bañados–Teitelboim–Zanelli (BTZ) black hole in (2+1)-dimensional spacetime. Due to the non-separability of the Klein–Gordon equation induced by the acceleration parameter, we employ an azimuthal-average approximation to derive an effective potential for massless scalar fields. In the low-frequency limit, we solve the radial equation using matched asymptotic expansions near the horizon and in the far region, accounting for rotation via the horizon angular velocity. Our results yield a power-law scaling for the greybody factor, $\Gamma(\omega) \propto (\omega - m\Omega_H)^{2\lambda-1}$, where $\lambda = \sqrt{\mu^2\ell^2 + 5/4}$, highlighting deviations from pure blackbody radiation. We discuss implications for Hawking radiation, superradiance in the regime $\omega < m\Omega_H$, and the role of acceleration in modifying black hole thermodynamics.

1 Introduction

Black holes are the most interesting objects in gravitational physics. They connect three major areas of science: general relativity, quantum mechanics, and thermodynamics. When black holes are considered as thermal systems, they are found to have entropy and emit Hawking radiation. This shows that black holes are not completely dark, they can release energy due to quantum effects [7,8,17,21,25,32]. These special features make black holes very important for studying how gravity and quantum field theory are compatible.

For simple fields like massless scalar fields, physicists have studied how black holes emit radiation and how greybody factors affect this process. These studies have explored different black holes: static, rotating, and in different backgrounds like flat space, de Sitter, and anti-de Sitter spacetimes [1,2,10,13,15,26,29,31,33]. In higher-dimensional theories, these calculations include both radiation trapped on a 4D brane [20,23,24] and radiation spreading in the full higher-dimensional space [19,22]. Special cases such as graviton emission have also been explored [11].

In lower dimensions, the Bañados–Teitelboim–Zanelli (BTZ) black hole is a very useful model. Even though it exists in only (2+1) dimensions, it still shares many important properties of higher-dimensional black holes, like horizons, thermodynamic laws, and Hawking radiation [5,6,12]. Adding acceleration and rotation to the BTZ black hole makes it an even richer system to study, while still being simple enough for detailed analysis [3,4].

Greybody factor play a key role in understanding how radiation escapes from black holes. In most cases, they are too hard to calculate exactly and require computer simulations. But in special situations, such as at very low frequencies where only the simplest wave (the S-wave with $\ell = 0$) is relevant, exact results can be obtained. This low-frequency limit is often used to study how black holes scatter incoming waves. Another exact method comes from hidden symmetries of non-rotating black holes, which are connected to the Korteweg–de Vries (KdV) equation. The conserved quantities of this equation, called KdV integrals, can fully determine the greybody factors in some cases [18,28].

Greybody factor is also important in astrophysics. It affects the gravitational wave signal which one observes when two black holes merge, especially in the ringdown phase. Unlike quasinormal modes, greybody factor do not change much if the shape of the black hole is slightly altered. Because of this stability, they are useful not only for studying Hawking radiation but also for interpreting gravitational wave data from real black holes in space [27,34].

A crucial element in the study of black hole radiation is the greybody factor, which modifies the spectrum of Hawk-

[a] e-mail: jamil.ahmed@fecid.paf-iast.edu.pk (corresponding author)
[b] e-mail: ugilani@nutech.edu.pk
[c] e-mail: mrehman@math.qau.edu.pk

Published online: 03 March 2026

ing radiation observed at infinity. While the emission near the event horizon is nearly thermal, the propagation of radiation through the curved spacetime leads to partial reflection by the effective potential barrier [16,30]. As a result, the spectrum deviates from that of a perfect blackbody. The greybody factor, denoted by $\gamma(\omega)$, quantifies this modification and thus plays a central role in bridging semiclassical predictions with observable radiation. In the semiclassical description, the average particle number at frequency ω takes the form

$$\langle n(\omega)\rangle = \frac{\gamma(\omega)}{e^{\omega/T_H} \pm 1}, \tag{1}$$

where T_H is the Hawking temperature and the $\pm$ sign corresponds to bosonic or fermionic statistics. In this work, we analyze the greybody factor for the accelerating rotating BTZ black hole. This case provides an opportunity to examine how acceleration and angular momentum affect the transmission of radiation through the black hole's potential barrier. The study not only deepens our understanding of Hawking radiation in lower dimensions but also offers insight into the role of additional geometric parameters in shaping black hole thermodynamics [9,14].

The paper is organised as follows: In Sect. 2, we introduce the metric for the accelerating and rotating BTZ. In Sect. 3, we derive analytical expression for effective potential and its graphical exploration. Finally in Sect. 4, computation of greybody factor is presented as a solution of Klein–Gorden equation in low-frequency limit. We conclude with some discussions at the end.

2 Metric of accelerating rotating BTZ

We consider a $(2+1)$-dimensional accelerating and rotating BTZ-like spacetime described by the conformally related metric

$$ds^2 = g_{\mu\nu}dx^\mu dx^\nu = \frac{1}{\Omega^2(\phi,r)} \times \left[-N^2(r)\,dt^2 + \frac{dr^2}{N^2(r)} + r^2\big(d\phi + N^\phi(r)\,dt\big)^2\right], \tag{2}$$

where the conformal factor

$$\Omega(\phi,r) = 1 + \alpha r\cos\phi \tag{3}$$

encodes the effect of acceleration through the parameter α. In the limit $\alpha \to 0$, the conformal factor reduces to unity and the metric smoothly recovers the standard rotating BTZ spacetime. The lapse function $N(r)$ and the angular shift $N^\phi(r)$ are given by

$$N^2(r) = -M + \frac{r^2}{\ell^2} + \frac{J^2}{4r^2}, \tag{4}$$

$$N^\phi(r) = -\frac{J}{2r^2}, \tag{5}$$

where M and J denote the mass and angular momentum of the black hole, respectively, and ℓ is the AdS length scale related to the cosmological constant by $\Lambda = -1/\ell^2$. The horizon structure of the spacetime is determined by the real positive roots of $N^2(r) = 0$.

To investigate the dynamics of a massive scalar field Φ propagating in this background, we consider the Klein–Gordon equation

$$\left(\Box_g - \mu^2\right)\Phi = 0, \tag{6}$$

where μ is the mass of the scalar field and $\Box_g$ denotes the covariant d'Alembertian operator associated with the metric $g_{\mu\nu}$. Explicitly, the Klein–Gordon operator can be written as

$$\mathcal{D}\Phi \equiv \frac{1}{\sqrt{-g}}\partial_\mu\left(\sqrt{-g}\,g^{\mu\nu}\partial_\nu\Phi\right) - \mu^2\Phi. \tag{7}$$

Since the spacetime metric $g_{\mu\nu}$ is conformally related to an ADM-type metric $h_{\mu\nu}$ via

$$g_{\mu\nu} = \Omega^{-2}h_{\mu\nu}, \tag{8}$$

the inverse metric and the determinant transform according to

$$g^{\mu\nu} = \Omega^2 h^{\mu\nu}, \qquad \sqrt{-g} = \Omega^{-3}\sqrt{-h}, \tag{9}$$

where the power of the conformal factor arises from the $(2+1)$-dimensional nature of the spacetime. Substituting these relations into Eq. (7), the Klein–Gordon operator can be expressed entirely in terms of the conformally related metric $h_{\mu\nu}$ as

$$\mathcal{D}\Phi = \frac{\Omega^3}{\sqrt{-h}}\partial_\mu\left(\Omega^{-1}\sqrt{-h}\,h^{\mu\nu}\partial_\nu\Phi\right) - \mu^2\Phi. \tag{10}$$

This form explicitly demonstrates how the conformal factor $\Omega(\phi,r)$ modifies the scalar field dynamics and shows that the effect of acceleration enters the Klein–Gordon equation solely through the conformal structure of the spacetime.

Expanding the derivative gives the explicit form

$$\frac{\Omega^3}{\sqrt{-h}}\partial_\mu\left(\Omega^{-1}\sqrt{-h}\,h^{\mu\nu}\partial_\nu\Phi\right) = \Omega^2\,h^{\mu\nu}\nabla^{(h)}_\mu\partial_\nu\Phi - \Omega^3 h^{\mu\nu}(\partial_\mu\Omega^{-1})\partial_\nu\Phi = 0, \tag{11}$$

where $\nabla^{(h)}$ is the covariant derivative with respect to $h_{\mu\nu}$. This form shows two new features compared with the $\Omega=1$ case, One of the case is an overall conformal rescaling of the kinetic operator by factor Ω^2. Second case is first-derivative terms proportional to gradients of $\Omega^{-1}(\phi, r)$ which depend on ϕ and thus spoil naive separability. The metric is $2\pi-$periodic in ϕ we expand the field in angular modes as

$$\Phi(t, r, \phi) = e^{-i\omega t} \sum_{m\in\mathbb{Z}} \psi_m(r)\, e^{im\phi}. \tag{12}$$

Substituting (12) into (7) and projecting onto the $e^{in\phi}$ Fourier component (multiply by $e^{-in\phi}$ and integrate $\phi \in [0, 2\pi]$) yields an infinite coupled system of radial ordinary differential equations for $\{\psi_m(r)\}$

$$\sum_{m\in\mathbb{Z}} \mathcal{L}_{nm}(r;\omega)\, \psi_m(r) = 0, \qquad n \in \mathbb{Z}, \tag{13}$$

where the radial differential operator matrix elements are

$$\mathcal{L}_{nm}(r;\omega) = \frac{1}{2\pi}\int_0^{2\pi} e^{-in\phi} \left\{ \frac{\Omega^3}{\sqrt{-h}}\partial_\mu \times \left(\Omega^{-1}\sqrt{-h}\, h^{\mu\nu}\partial_\nu\left(e^{im\phi}e^{-i\omega t}\right)\right) - \mu^2 e^{im\phi}e^{-i\omega t}\right\} d\phi. \tag{14}$$

All ϕ-dependence is contained in explicit factors of $\Omega(\phi, r)$ and its derivatives; evaluating the integral produces coupling coefficients between modes m and n (in particular $m \leftrightarrow m \pm 1$ couplings arise because $\cos\phi$ appears in Ω). After carrying out the t, ϕ derivatives acting on the exponentials and performing the ϕ-projection one may cast (13) in the schematic form

$$\sum_{m\in\mathbb{Z}} \left\{ \mathcal{A}_{nm}(r)\, \frac{d^2\psi_m}{dr^2} + \mathcal{B}_{nm}(r)\, \frac{d\psi_m}{dr} + \mathcal{C}_{nm}(r;\omega)\, \psi_m(r)\right\} = 0, \tag{15}$$

where the coefficient matrices $\mathcal{A}, \mathcal{B}, \mathcal{C}$ are explicit functions of r built from $N^2(r)$, $N^\phi(r)$ and the Fourier components of Ω^{-1}, Ω^{-3} and their r-derivatives. In particular $\mathcal{C}_{nm}$ contains terms proportional to $(\omega + m\bar{N}^\phi(r))(\omega + n\bar{N}^\phi(r))$ appropriately weighted by Fourier overlaps, where $\bar{N}^\phi(r)$ is the m-averaged frame dragging. The coupling coefficients are given by Fourier integrals of the form as

$$\mathcal{F}_k(r) \equiv \frac{1}{2\pi}\int_0^{2\pi} \frac{e^{-ik\phi}}{1+\alpha r\cos\phi}\, d\phi\,, \quad k \in \mathbb{Z}. \tag{16}$$

These coefficients determine how mode m couples to mode n with $k = n - m$. The integral (16) can be evaluated in closed form by contour integration and will have the form

$$\mathcal{F}_k(r) = \frac{1}{\sqrt{1-\beta^2}} \left(\frac{1-\sqrt{1-\beta^2}}{\beta}\right)^{|k|}, \quad \beta = \alpha r, \tag{17}$$

which shows exponential decay of coupling strength with $|k|$ when $|\beta| < 1$ and oscillatory/growing behaviour when $|\beta| > 1$.

3 Effective potential for the accelerating rotating BTZ black hole

For the full conformal metric (2) with the Klein–Gordon equation for a mode

$$\Phi(t, r, \phi) = e^{-i\omega t} e^{im\phi} R(r), \tag{18}$$

cannot be separated exactly because Ω depends on ϕ, which couples different azimuthal Fourier modes. A common simplification is to *project* the full equation onto a single mode m by averaging over ϕ, i.e.

$$\langle X(r,\phi)\rangle_\phi \equiv \frac{1}{2\pi}\int_0^{2\pi} X(r,\phi)\, d\phi, \tag{19}$$

which removes the explicit ϕ-dependence in coefficients while keeping the full r-dependence. This produces a single radial equation for $R(r)$

$$R''(r) + P(r)R'(r) + Q(r)R(r) = 0, \tag{20}$$

where $P(r)$ and $Q(r)$ are the ϕ-averaged coefficients obtained from the full Klein–Gordon operator. The Schrödinger-like form is obtained by defining

$$\psi(r) = e^{-\frac{1}{2}\int^r P(s)\, ds}\, R(r), \tag{21}$$

which eliminates the first derivative term, yielding

$$\psi''(r) + \left[\omega_{\text{eff}}^2(r) - V_{\text{eff}}(r)\right]\psi(r) = 0, \tag{22}$$

where in this approximation $\omega_{\text{eff}}(r) = \omega + m\langle N^\phi(r)\rangle_\phi$ and the effective potential is

$$V_{\text{eff}}(r) = -Q(r) + \frac{1}{2}P'(r) + \frac{1}{4}P(r)^2. \tag{23}$$

This potential is not exact for the accelerating rotating BTZ black hole; it neglects couplings between different m

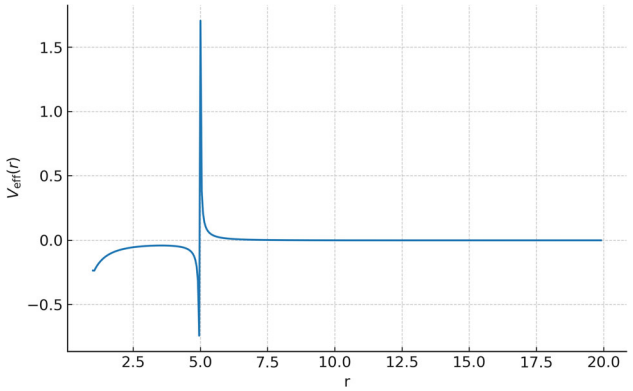

Fig. 1 The plot shows $V_{\text{eff}}(r)$ for sample parameters $M = 1.0$, $J = 0.5$, $\ell = 5.0$, $\alpha = 0.05$, $\mu = 0.1$, $m = 0$, using the azimuthal-average approximation

modes induced by $\Omega(\phi, r)$. It is, however, a useful tool for visualizing the main radial barrier structure.

The behavior of the effective potential $V_{\text{eff}}(r)$ is illustrated in Fig. 1 for representative values of the black hole parameters. A pronounced divergence appears in the vicinity of the event horizon, indicating the formation of a strong potential barrier generated by the combined effects of black hole rotation and acceleration. This barrier partially reflects the outgoing scalar modes and allows only a fraction of the Hawking radiation to reach asymptotic infinity, thereby playing a decisive role in determining the greybody factor through the associated transmission and reflection coefficients. At large radial distances, the effective potential gradually decays to zero, which is consistent with the asymptotically AdS structure of the spacetime and permits free propagation of scalar waves in the far-field region.

4 Solution of the radial Klein–Gordon equation and the low-frequency greybody factor

We work in the azimuthal-diagonal (single-mode) azimuthal-average approximation described earlier, where the Klein-Gorden radial equation is written in Schrödinger-like form

$$\frac{d^2\psi}{dr_*^2} + \left[\left(\omega + mN^{\phi}(r)\right)^2 - V_{\text{eff}}(r)\right]\psi = 0, \tag{24}$$

with r_* the tortoise coordinate defined by $dr_*/dr = 1/N^2(r)$ and the effective potential $V_{\text{eff}}(r)$ is given in the previous section. We denote the horizon radius by r_h (the largest root of $N^2(r_h) = 0$), the surface gravity by $\kappa = \frac{1}{2}N^{2\prime}(r_h)$, and the horizon angular velocity by

$$\Omega_H \equiv -N^{\phi}(r_h) = \frac{J}{2r_h^2}.$$

Near the event horizon $r \to r_h$ we expand

$$N^2(r) \approx 2\kappa(r - r_h), \quad N^{\phi}(r) \approx N^{\phi}(r_h) = -\Omega_H.$$

The tortoise coordinate behaves as $r_* \simeq \frac{1}{2\kappa}\ln(r - r_h)$, so the dominant near-horizon equation (24) reduces to

$$\frac{d^2\psi}{dr_*^2} + (\omega - m\Omega_H)^2\psi \simeq 0.$$

The general near-horizon solution is therefore

$$\psi_{\text{NH}}(r_*) = A_{\text{in}}\, e^{-i(\omega - m\Omega_H)r_*} + A_{\text{out}}\, e^{+i(\omega - m\Omega_H)r_*}.$$

Imposing the physical ingoing boundary condition (regular on the future horizon) sets $A_{\text{out}} = 0$, hence

$$\psi_{\text{NH}}(r) \simeq A_{\text{in}}\,(r - r_h)^{-i(\omega - m\Omega_H)/(2\kappa)}. \tag{25}$$

For far-region solution $r \gg r_h$ (and in particular for $r \gg \ell\sqrt{M}$ but still $r \ll 1/\omega$ in the matching region) the AdS asymptotics dominate and the effective potential grows as $V_{\text{eff}}(r) \sim \dfrac{\lambda^2}{\ell^2}r^2$ with

$$\lambda \equiv \sqrt{\mu^2\ell^2 + \frac{5}{4}}.$$

Thus the far-region radial equation admits power-law solutions of the form

$$\psi_{\text{far}}(r) = C_1\, r^{\lambda} + C_2\, r^{-\lambda},$$

where $C_{1,2}$ are integration constants. The $r^{-\lambda}$ mode is the normalizable/decaying branch at spatial infinity in AdS and therefore corresponds to outgoing flux at infinity for scattering computations.

For matching in the overlap region $r_h \ll r \ll 1/\omega$ we may approximate $(r - r_h) \simeq r$ and expand the near-horizon solution (25) as a power of r:

$$\psi_{\text{NH}}(r) \simeq A_{\text{in}}\, r^{-i\varepsilon}, \quad \varepsilon \equiv \frac{\omega - m\Omega_H}{2\kappa} \ll 1.$$

We match this to the far solution

$$A_{\text{in}}\, r^{-i\varepsilon} \simeq C_1 r^{\lambda} + C_2 r^{-\lambda},$$

in the sense of asymptotic expansions in the small parameter ε and small frequency. The matching procedure yields that the decaying coefficient C_2 is proportional to A_{in} times a positive power of $(\omega - m\Omega_H)$

$$C_2 \propto A_{\text{in}}\,(\omega - m\Omega_H)^{\lambda}.$$

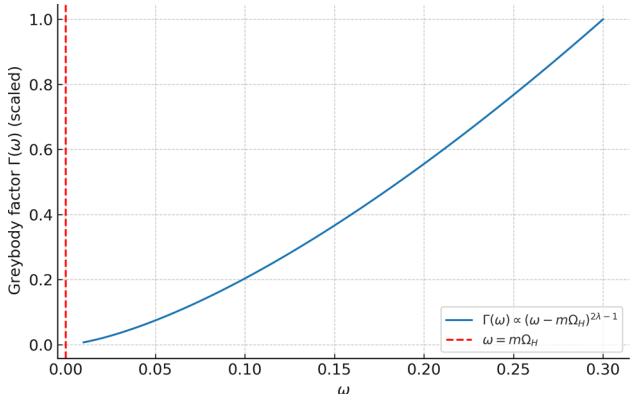

Fig. 2 The plot illustrates the scaling for sample parameters $M = 1.0$, $J = 0.5$, $\ell = 5.0$, $\alpha = 0.05$, $\mu = 0.1$, $m = 0$

A straightforward power-counting gives the low-frequency scaling of the transmitted amplitude; squaring the amplitude gives the greybody factor scaling.

The greybody factor (transmission coefficient) is the ratio of outgoing flux at infinity to ingoing flux at the horizon

$$\Gamma(\omega) \equiv \frac{F_\infty}{F_{\rm hor}} = \frac{\text{const} \times |C_2|^2}{(\omega - m\Omega_H)\,|A_{\rm in}|^2}.$$

Using the matched-scaling $|C_2|^2 \propto |A_{\rm in}|^2(\omega - m\Omega_H)^{2\lambda}$ we obtain the characteristic low-frequency power-law behaviour

$$\Gamma(\omega) \;\propto\; (\omega - m\Omega_H)^{2\lambda-1} \quad (\omega \ll 1/\ell,\ \text{diagonal approx.}), \tag{26}$$

where $\lambda = \sqrt{\mu^2\ell^2 + 5/4}$. we observe the following points, for the non-rotating case ($J = 0$ so $\Omega_H = 0$) this reduces to the familiar scaling $\Gamma \propto \omega^{2\lambda-1}$. When $\omega > m\Omega_H$ the horizon flux is positive and $\Gamma(\omega) > 0$; when $\omega < m\Omega_H$ the horizon flux changes sign and the scattering is superradiant: the reflected flux at infinity can be larger than the incident flux.

For $\omega > m\Omega_H$ the greybody factor rises as a power law with exponent $2\lambda - 1$. At $\omega = m\Omega_H$ the curve starts from zero, consistent with the ingoing flux boundary condition. For $\omega < m\Omega_H$ the superradiant regime occurs, where the transmission coefficient can formally exceed unity. The vertical dashed line marks $\omega = m\Omega_H$, separating the superradiant and non-superradiant regimes.

Figure 2 depicts the frequency dependence of the greybody factor $\Gamma(\omega)$ for scalar wave propagation in an accelerating and rotating BTZ black hole background, evaluated for representative values of the system parameters. The greybody factor vanishes at the threshold frequency $\omega = m\Omega_H$, marked by the vertical dashed line, reflecting the absence of wave transmission below this critical value due to the combined effects of rotation and acceleration. As the frequency increases beyond the threshold, $\Gamma(\omega)$ rises monotonically, indicating an enhanced transmission probability of scalar modes through the effective potential barrier. This behavior demonstrates that higher-frequency modes are less affected by the barrier structure and can escape more efficiently to infinity. The observed scaling of the greybody factor highlights the role of acceleration and rotation in modulating the spectral distribution of Hawking radiation emitted by the accelerating rotating BTZ black hole.

5 Conclusion

In this work, we have analyzed the greybody factor of an accelerating and rotating BTZ black hole by employing an azimuthal-average approximation to overcome the difficulties arising from the nonseparability of the Klein–Gordon equation. By deriving the corresponding effective potential and solving the radial equation in the low-frequency regime, we obtained an analytical expression for the greybody factor,

$$\Gamma(\omega) \propto (\omega - m\Omega_H)^{2\lambda-1},$$

which explicitly encodes the influence of black hole acceleration, rotation, and the AdS length scale. This scaling behavior reveals key physical features, including the onset of superradiance for $\omega < m\Omega_H$ and the stability of scalar perturbations in the non-superradiant regime, thereby providing deeper insight into radiation propagation in curved lower-dimensional spacetimes.

The behavior of the effective potential $V_{\rm eff}(r)$ is illustrated in Fig. 1 for representative values of the black hole parameters. A pronounced divergence is observed in the vicinity of the event horizon, signaling the formation of a strong potential barrier generated by the combined effects of black hole rotation and acceleration. This barrier partially reflects the outgoing scalar modes, allowing only a fraction of the Hawking radiation to reach asymptotic infinity. Consequently, the effective potential plays a decisive role in determining the greybody factor through the associated transmission and reflection coefficients. At large radial distances, $V_{\rm eff}(r)$ gradually decays to zero, consistent with the asymptotically AdS structure of the spacetime, which permits free propagation of scalar waves in the far-field region.

Figure 2 depicts the frequency dependence of the greybody factor $\Gamma(\omega)$ for scalar wave propagation in an accelerating and rotating BTZ black hole background, evaluated for representative values of the system parameters. The greybody factor vanishes at the threshold frequency $\omega = m\Omega_H$, indicated by the vertical dashed line, reflecting the absence of wave transmission below this critical value due to the combined influence of rotation and acceleration. For frequencies exceeding the threshold, $\Gamma(\omega)$ increases monotonically,

demonstrating an enhanced transmission probability of scalar modes through the effective potential barrier. This behavior indicates that higher-frequency modes are less sensitive to the barrier structure and can escape more efficiently to infinity. Overall, the observed scaling of the greybody factor highlights the crucial role played by acceleration and rotation in shaping the spectral distribution of Hawking radiation emitted by accelerating rotating BTZ black holes.

Our results bridge semiclassical predictions with observable spectral characteristics and underscore the importance of geometric parameters in black hole thermodynamics. Future studies could extend the present analysis to include full mode coupling, higher-frequency regimes, or fermionic fields, which would allow for a refinement of numerical prefactors and provide further insight into broader theoretical and astrophysical implications.

Data Availability Statement This manuscript has no associated data. [Authors' comment: No data was used for the research described in the article.]

Code Availability Statement This manuscript has no associated code/software. [Authors' comment: No code was used for the research described in the article.]

Funded by SCOAP[3].

References

1. J. Ahmed, K. Saifullah, Eur. Phys. J. C **77**, 885 (2017)
2. J. Ahmed, K. Saifullah, Eur. Phys. J. C **78**, 316 (2018)
3. M. Astorino, JHEP **01**, 114 (2011)
4. M. Astorino, Phys. Rev. D **88**, 104027 (2013)
5. M. Bañados, C. Teitelboim, J. Zanelli, Phys. Rev. Lett. **69**, 1849 (1992)
6. M. Bañados, M. Henneaux, C. Teitelboim, J. Zanelli, Phys. Rev. D **48**, 1506 (1993)
7. J.M. Bardeen, B. Carter, S. Hawking, Commun. Math. Phys. **31**, 161 (1973)
8. J.D. Bekenstein, Phys. Rev. D **7**, 2333 (1973)
9. D. Birmingham, I. Sachs, S.N. Solodukhin, Phys. Rev. Lett. **88**, 151301 (2002)
10. P. Boonserm, M. Visser, Phys. Rev. D **78**, 101502 (2008)
11. V. Cardoso, M. Cavaglia, L. Gualtieri, JHEP **02**, 021 (2006)
12. S. Carlip, Class. Quantum Gravity **12**, 2853 (1995)
13. B. Carneiro da Cunha, F. Novaes, Phys. Rev. D **93**, 024045 (2016)
14. J. Crisóstomo, S. Lepe, J. Saavedra, Class. Quantum Gravity **21**, 2801 (2004)
15. L.C.B. Crispino, A. Higuchi, E.S. Oliveira, J.V. Rocha, Phys. Rev. D **87**, 104034 (2013)
16. S.R. Das, G. Gibbons, S.D. Mathur, Phys. Rev. Lett. **78**, 417 (1997)
17. A. Ejaz, H. Gohar, H. Lin, K. Saifullah, S.T. Yau, Phys. Lett. B **726**, 827 (2013)
18. J. Grain, Phys. Rev. D **72**, 104016 (2005)
19. T. Harmark, J. Natario, R. Schiappa, Adv. Theor. Math. Phys. **14**, 727 (2010)
20. C.M. Harris, P. Kanti, JHEP **10**, 014 (2003)
21. V. Cardoso, M. Cavaglia, L. Gualtieri, JHEP **02**, 021 (2006)
22. R. Jorge, E.S. de Oliveira, J.V. Rocha, Class. Quantum Gravity **32**, 065008 (2015)
23. P. Kanti, J. March-Russell, Phys. Rev. D **66**, 024023 (2002)
24. P. Kanti, T. Pappas, N. Pappas, Phys. Rev. D **90**, 124077 (2014)
25. R. Kerner, R.B. Mann, Class. Quantum Gravity **25**, 095014 (2008)
26. J.M. Maldacena, A. Strominger, Phys. Rev. D **56**, 4975–4983 (1997)
27. F. Moura, JHEP **1309**, 038 (2013)
28. F. Moura, R. Schiappa, Class. Quantum Gravity **24**, 361 (2007)
29. D.N. Page, Phys. Rev. D **14**, 3260–3273 (1976)
30. D.N. Page, Phys. Rev. D **13**, 198 (1976)
31. D.N. Page, Phys. Rev. D **13**, 198–206 (1976)
32. M.K. Parikh, F. Wilczek, Phys. Rev. Lett. **85**, 5042 (2000)
33. D. Birmingham, I. Sachs, S.N. Solodukhin, Phys. Rev. Lett. **88**, 151301 (2002)
34. C.Y. Zhang, P.C. Li, B. Chen, Phys. Rev. D **97**, 044013 (2018)